Multi-Instrument Observations of Geomagnetic Storms in the Arctic Ionosphere

Tibor Durgonics*[1,2], Attila Komjathy[1,3], Olga Verkhoglyadova[1], Esayas B. Shume[1,4], Hans-Henrik Benzon[2], Anthony J. Mannucci[1], Mark D. Butala[5], Per Høeg[2], and Richard B. Langley[3]

[1] NASA Jet Propulsion Laboratory, Pasadena, CA, USA.
(E-mail: tibdu@space.dtu.dk*)
[2] Technical University of Denmark, National Space Institute (DTU Space), Kongens Lyngby, Denmark.
[3] Dept. of Geodesy and Geomatics Engineering, University of New Brunswick, Fredericton, N.B., Canada.
[4] Astronomy Department, Caltech, Pasadena, CA, USA.
[5] University of Illinois at Urbana-Champaign, Champaign, IL, USA.

ABSTRACT

We present a multi-instrumented approach for the analysis of the Arctic ionosphere during the 19 February 2014 highly complex, multiphase geomagnetic storm. The geomagnetic storm was the result of two powerful and subsequent Earth-directed coronal mass ejections (CMEs). The first one was launched from the solar corona on 16 February and the second one on 18 February. We focus on effects of such solar-originated geomagnetic disturbances on the high latitude ionosphere because our present understanding of the fundamental ionospheric processes – particularly during perturbed times – in this region is still incomplete.

We employ GNSS networks, geomagnetic observatories, and a specific ionosonde station in Greenland and complementary data with spaceborne measurements in order to map the state and variability of the Arctic ionosphere. Due to the fact that all the ground-based measurements used in this work were collected in Greenland the focus remains on the Greenland sector of the Arctic ionosphere (Figure 1, left panel). The sheer size and location of Greenland allow ground-based measurements stretching from the deep polar cap to the equatorward edge of the auroral oval making it possible to compare directly disparate regions (Figure 1, right panel). The ionospheric GNSS-based total electron content (TEC) values [1] augmented with ionosonde-derived vertical electron density (Ne) profiles revealed negative storm phases, following the first CME commencement, which lasted for several days.

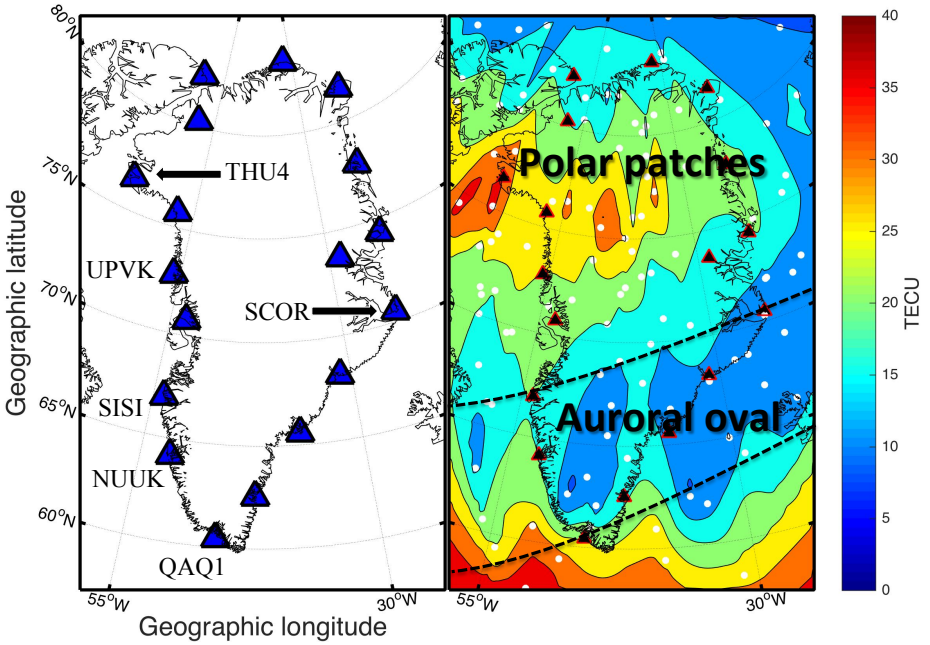

Figure 1. (left-panel) Map of Greenland with blue triangles marking the locations of a subset of Greenland GNSS stations that have been employed to generate the VTEC maps in this study. Six out of the 18 stations were specifically labeled so their locations will be easily identified in later figures. Legend for the station codes are as follows: Nuuk (NUUK), Qaqortoq (QAQ1), Scorebysund (SCOR), Sisimiut (SISI), Thule (THU4), Upernavik (UPVK). (right-panel) VTEC map over Greenland at 19:15:00 (UTC), 18 February 2014. The VTEC values at the ionospheric pierce points are denoted with white circles.

During this phase thermospheric O/N_2 measurements [2] demonstrated significantly lower values over the Greenland sector than prior to the storm-time and the composition changes resulted in F-region depletion. Analysis of changes in the disturbance storm-time (Dst) index, auroral electrojet (AE) index, and northern polar cap index (PCN) indicated that the negative storm depletion is the direct consequence of energy input into the polar cap [3]. The Canadian CASSIOPE (CAScade Smallsat and IOnospheric Polar Explorer) multi-mission satellite's ion mass spectrometer (IRM) measured an increased ion flow in the topside ionosphere during the negative storm phase [4], which supports the notion that Joule heating may have caused the composition change. Polar patch generation was significantly decreased during the negative storm phase. The patches were clearly identifiable by employing the rate of TEC index (ROTI) even under superimposed solar-induced TEC gradient conditions [5].

Based on the multiple instrument observation approach and analyses technique, we present the physical processes that may be responsible for ionospheric storm development in the northern high-latitudes.

Key words: Total electron content, Scintillations, GNSS, Ionograms, Geomagnetic storms, High-latitude ionosphere.

References

[1] Hernandez-Pajares, M., J. M. Juan, J. Sanz, and R. Orus (2007), Second-order ionospheric term in GPS: Implementation and impact on geodetic estimates, Journal of Geophysical Research, 112, B08417, doi:10.1029/2006JB004707.

[2] Verkhoglyadova, O.P., B. T. Tsurutani, A. J. Mannucci, M. G. Mlynczak, L. A. Hunt, and L. J. Paxton (2014), Ionospheric TEC, thermospheric cooling and $\Sigma[O/N_2]$ compositional changes during the 6–17 March 2012 magnetic storm interval (CAWSES II), Journal of Atmospheric and Solar-Terrestrial Physics, Vol 115–116, spp. 41–51, doi:10.1016/j.jastp.2013.11.009.

[3] Vennerstrøm, S., E. Friis-Christensen, O. A. Troshichev, and V. G. Andersen (1991), Comparison between the polar cap index, PC, and the auroral electrojet indices AE, AL, and AU, J. Geophys. Res., 96(A1), 101–113, doi:10.1029/90JA01975.

[4] Yau, A. W., A. Howarth, A. White, G. Enno, and P. Amerl (2015) Imaging and Rapid-Scanning Ion Mass Spectrometer (IRM) for the CASSIOPE e-POP mission, Space Science Reviews, 189, pp. 41-63, doi:10.1007/s11214-015-0149-8.

[5] Pi, X., A. J. Mannucci, B. Valant-Spaight, Y. Bar-Sever, L. J. Romans, S. Skone, L. Sparks, and G. Martin Hall (2013), Observations of global and regional ionospheric irregularities and scintillation using GNSS tracking networks, Proceedings of the ION 2013 Pacific PNT Meeting, Honolulu, Hawaii, April 2013, pp. 752-761.

Acknowledgements

The authors wish to thank Lowell Digisonde International for providing access to Thule digisonde data used in this work; The Greenland GPS Network (GNET) operated by the Technical University of Denmark, National Space Institute (DTU Space) in cooperation with the American National Science Foundation, Ohio State University, and the non-profit university governed consortium UNAVCO for GPS data; The Technical University of Denmark, National Space Institute's Geomagnetism Section for magnetometer observations. We are grateful to NASA Jet Propulsion Laboratory for GIM data processing.

The Global Ultraviolet Imager (GUVI) data used here are provided through support from the NASA MO&DA program. The GUVI instrument was designed and built by The Aerospace Corporation and The Johns Hopkins University. The Principal Investigator is Dr. Andrew B. Christensen and the chief scientist and co-PI is Dr. Larry J. Paxton.

The authors also acknowledge the use of SuperDARN convection data and CASSIOPE IRM sensor data from e-POP.

Data used in this paper may be obtained from the authors.